Journal of Biomechanics 99 (2020) 109552

Contents lists available at ScienceDirect

Journal of Biomechanics

journal homepage: www.elsevier.com/locate/jbiomech
www.JBiomech.com

Effects of segment masses and cut-off frequencies on the estimation of vertical ground reaction forces in running

Dimitrios-Sokratis Komaris [a,*], Eduardo Perez-Valero [a], Luke Jordan [b], John Barton [a], Liam Hennessy [b], Brendan O'Flynn [a], Salvatore Tedesco [a]

[a] Tyndall National Institute, University College Cork, Lee Maltings Complex, Dyke Parade, T12R5CP Cork, Ireland
[b] Setanta College Ltd, Thurles Chamber Enterprise Ireland, Nenagh Road, Thurles, Ireland

ARTICLE INFO

Article history:
Accepted 29 November 2019

Keywords:
Impact forces
Running performance
Wearable sensors
Accelerometry
Kinetics
Biomechanical modelling

ABSTRACT

The purpose of this study is to examine the effect of the body's mass distribution to segments and the filtering of kinematic data on the estimation of vertical ground reaction forces from positional data. A public dataset of raw running biomechanics was used for the purposes of the analysis, containing recordings of twenty-eight competitive or elite athletes running on an instrumented treadmill at three different speeds. A grid-search on half of the trials was employed to seek the values of the parameters that optimise the approximation of biomechanical loads. Two-way ANOVAs were then conducted to examine the significance of the parameterised factors in the modelled waveforms. The reserved recordings were used to validate the predictive accuracy of the model. The cut-off filtering frequencies of the pelvis and thigh markers were correlated to running speed and heel-strike patterns, respectively. Optimal segment masses were in agreement with standardised literature reported values. Root mean square errors for slow running (2.5 m/s) were on average equal to 0.1 (body weight normalized). Errors increased with running speeds to 0.13 and 0.18 for 3.5 m/s and 4.5 m/s, respectively. This study accurately estimated vertical ground reaction forces for slow-paced running by only considering the kinematics of the pelvis and thighs. Future studies should consider configuring the filtering of kinematic inputs based on the location of markers and type of running.

1. Introduction

The study of ground reaction forces (GRFs) in running is commonly employed to enhance athletes' performance (e.g. Kawamori et al., 2013), determine injury-related factors (e.g. Bates et al., 2013), and evaluate the outcome of rehabilitation programs (e.g. Chmielewski et al., 2006). Accurate measurements are currently limited to laboratory settings, where trials are captured by optoelectronic systems, and embedded force platforms or instrumented treadmills. Yet, such methods require highly trained operators, are costly and demand dedicated spaces. Additionally, with respect to the utility of force plates, the analysis is commonly narrowed to a single gait cycle.

In an effort to accurately gauge biomechanical loads on open field, techniques have been developed to either directly measure or estimate running GRFs by means of wearable sensors. Overall, such approaches may be classified into three categories (Ancillao et al., 2018): direct force measurements with wearable load-cells (e.g. Liedtke et al., 2007; Tao et al., 2012), indirect methods with wearable pressure insoles (e.g. Shu et al., 2010; Crea et al., 2014), and techniques that approximate forces from body kinematics (e.g. Bobbert et al., 1991; Ohtaki et al., 2001; Clark et al., 2017; Verheul et al., 2018). Even though direct approaches with force sensors are the most accurate, they are generally bulky, costly, high-energy consuming, and impractical due to their altered contact interface between the feet and the ground (Liedtke et al., 2007; Jacobs & Ferris, 2015). Pressure insoles have also been shown to estimate anterior-posterior and vertical GRFs with very good accuracy (Forner Cordero et al., 2004; Fong et al., 2008); nonetheless, they are still accompanied with practical long-term considerations due to their short lifespan (Shahabpoor & Pavic, 2017), rapid degradation, and feebleness (El Kati et al., 2010). Contrarily, GRF estimation based on kinematics is currently the least accurate but has the highest potential for applicability. The capacity of a model relying on a kinematics to predict GRFs depends on whether the data were obtained by optoelectronics (e.g. Bobbert et al.,

* Corresponding author at: Tyndall National Institute, University College Cork, Lee Maltings, Dyke Parade, T12 R5CP Cork, Ireland.
E-mail address: sokratis.komaris@tyndall.ie (D.-S. Komaris).

https://doi.org/10.1016/j.jbiomech.2019.109552
0021-9290/

1991; Ren et al., 2008; Fluit et al., 2014; Clark et al., 2017) or inertial measurement units (IMUs) (e.g. Raper et al., 2018; Shahabpoor & Pavic, 2018), the number of sensors being used (Verheul et al., 2018), and its computational approach; for example, authors previously employed biomechanical models (e.g. Bobbert et al., 1991; Clark et al., 2017; Gurchiek et al., 2017; Verheul et al., 2018), neural networks (e.g. Kohle et al., 1997; Oh et al., 2013; Ngoh et al., 2018; Komaris et al., 2019), or mass-spring-damper systems (e.g. Nikooyan & Zadpoor, 2011; Nedergaard et al., 2018).

The development of low-cost and accessible wearable IMUs (Tedesco et al., 2016) led to the extensive validation of approaches drawing on kinematics with increasingly accurate results; for example, Karatsidis et al. (2016) demonstrated that the estimation of GRFs in walking using IMUs was comparable to studies using similar inputs from optoelectronic motion capture systems. As a general rule, biomechanical models commence by measuring segmental centre of mass (COM) accelerations, and subsequently estimate GRFs as the sum of products of segmental masses and accelerations. To the best of the authors' knowledge, the entirety of these works cope with the body's mass distribution in segments by adhering to literature data on average magnitudes of segment masses (e.g. Clauser et al., 1969; Dainis, 1980; De Leva, 1996; Winter, 2009). Yet, such approximations overlook the potential effect of the inherent variability in such measurements associated with each individual's mass distribution. Furthermore, low-pass filters are customarily used on kinematic data to prevent excessive noise; yet, authors rarely consider the effect of cut-off frequencies (f_c) on the high-frequency components of the recorded signal, particularly in high impact movements (e.g. Bobbert et al., 1991; Verheul et al., 2018).

Even though it is still arguable if segmental kinematics can be successfully used to predict GRFs during high impact activities (Verheul et al., 2018), the suggested approach may potential lead to improved modeling accuracy. Along these lines, the purpose of this work was to determine the optimal f_c and mass distribution on the approximation of GRFs in running. It was hypothesised that the f_c of the employed filter would increase with running speed since the acquired signal has higher frequency content; additionally, it was hypothesized that the optimised masses of the considered segments would be unrelated to running speed.

2. Methodology

2.1. Participants and data collection

A public dataset of raw running biomechanics, available at Figshare (DOI: https://doi.org/10.6084/m9.figshare.4543435), was used for this analysis (Fukuchi et al., 2017). The dataset contains trials of 28 regular runners (age: 34.8 ± 6.6 years; height: 176 ± 6.7 cm; mass: 69.6 ± 7.6 kg; gender: 27 males), with a training running volume greater than 20 km per week. Inclusion criteria included a minimum average running pace of 12 km/h during 10 km races and familiarity with treadmill running; participants with neurological or musculoskeletal disorders were excluded from the study. All participants were self-assessed to perform on either competitive or elite level.

Forty-eight technical and anatomical reflective markers were attached to the lower extremities and pelvis of each participant. Running trials were captured by 12 Raptor-4 motion cameras (Motion Analysis, Santa Rosa, CA, USA) and a Bertec dual-belt instrumented treadmill (Columbus, OH, USA) with sampling frequencies of 150 and 300 Hz, respectively. Three trials per participant of 30 s each, at 2.5, 3.5, and 4.5 m/s were logged. Additionally, the authors of the study used the centre of pressure and heel positions at heel-strike to identify foot-strike patterns. All recorded stances were considered in this analysis.

3. Data processing

Thigh and pelvis markers were singled from the dataset and further post-processed in Vicon Nexus (Oxford, UK). Gaps in the trajectories of four-marker cluster sets were treated with rigid body fills; gaps of 7 frames or smaller were filled with cubic spline interpolations; larger gaps were handled with either pattern or cyclic fills. Only the trajectories of the pelvis markers (left and right bony projections of the anterior and posterior superior iliac spine) and thigh markers (four-marker cluster sets, lateral mid-thighs) were further used.

Eighty-four trials in total (28 participants, 3 running speeds) containing spatial and force data were processed in MATLAB (MathWorks, MA, USA). Forces were filtered using a low-pass, second-order, zero-phase shift Butterworth filter with an f_c of 25 Hz. Positional data were up-sampled to 300 FPS to reach the sampling frequency of the instrumented treadmill. Subsequently, the dataset was divided into two equal parts; the first batch of trials (subjects $1-14$) was used for a grid-search to identify the combination of segment masses and f_c for the filtering of positional data that optimises the calculation of GRFs. The identified optimum parameters were then used in the latter part of the dataset (subjects $15-28$).

During the grid-search, positional time series were treated with the same filter that was used for the force data but with a broad range of f_c: $4-15$ Hz for the pelvis and $10-30$ Hz for the thigh markers, with 1Hz intervals. The thigh mass was also parameterised (m_{thigh}) with values extending from $8-28\%$ of the participant's total body mass (BM), with 1% increments (approximately equal to ±10% of the total mass of the entire lower-limb). As a result, a total of 5292 unique combinations per trial were analysed at this stage. Following the filtering process, and for each recording, the vertical positions of the pelvis and thigh marker subsets were averaged separately and double differentiated, resulting in an approximation of the segments' COM vertical acceleration (a_{pelvis} and a_{thigh}). The vertical components of the GRFs were then estimated as the summation of two products of masses and accelerations:

$$GRF_{vertical,estimated} = m_{thigh} \cdot (a_{thigh} + g) + m_{RBM} \cdot (a_{pelvis} + g) \quad (1)$$

$$m_{RBM} = BM - m_{thigh} \quad (2)$$

where g equals the gravitational acceleration, while the remaining body masses (m_{RBM}) are given by the difference between body and thigh masses (Eq. (2)). The combination of the three parameters that minimises the root mean square error ($RMSE_{BW}$, body weight normalised) between the actual force waveforms and those returned by the grid-search were then used to estimate GRFs (Eq. (1)) for the second portion of the dataset (subjects $15-28$).

3.1. Statistics

Two-way ANOVAs were conducted to examine the effect of running speed and foot-strike pattern on the f_c and thigh masses that minimised the RMSE statistic. In regards to the type of foot-strike, the performance of the dominant leg (subjects' self-reported) was used to dichotomise the dataset into forefoot and rearfoot groups. To validate the accuracy of our model, RMSE and goodness-of-fit (R^2) agreements, along with the difference in normalised absolute peak forces, were measured for the second half of the dataset and compared to the corresponding values from the grid-search. Statistical significance was set at $p < 0.05$ for all calculations.

Table 1
Grid-search parameters and errors (SD).

	Pelvis f_c *Hz*	Thigh f_c *Hz*	m_{thigh} *%BM*	*RMSE* *BW*	Absolute peak error *BW*	R^2
2.5 m/s	**5.7 (1.2)**	22.6 (5.3)	15 (4)	0.09 (0.02)	0.05 (0.04)	0.99
3.5 m/s	6.4 (1.6)	24.5 (5.5)	13 (3)	0.13 (0.03)	0.06 (0.04)	0.99
4.5 m/s	**7.4 (1.8)**	23.7 (5.3)	13 (3)	0.17 (0.03)	0.09 (0.05)	0.99
All speeds, m/s	6.5 (1.7)	23.6 (5.3)	14 (3)	0.13 (0.04)	0.07 (0.04)	0.99

In bold: statistically significant values ($p < 0.05$).

4. Results

The capacity of the grid-search to adequately approximate the sought waveforms diminishes linearly at higher running speeds (RMSE, Table 1). Goodness-of-fit statistic was identical across all running conditions ($R^2 = 0.99$). Similarly to the RMSE measurement, absolute peak error values (BW normalised) deteriorate with increasing speeds. Across all recordings, the highest peak error between modeled and observed forces for a single trial (mean for approximately 90 strides) was 115 N (data not shown).

Evidently, the optimum f_c of the pelvis markers increases with running speed (Table 1); yet, thigh f_c and mass appear to be unaffected by the same factor. Two-way ANOVAs were conducted to examine the effect of running speed and foot-strike pattern on f_c and mass allocation. There were no significant outliers within the data, while Shapiro-Wilk and Levene's test for homogeneity confirmed that the variables were generally normally distributed with homogeneous variances. The main effect of running speed on the optimum pelvis f_c was statistically significant ($p = 0.03$); as was the effect of foot-strike type on the f_c of the thighs ($p = 0.04$). There was no statistically significant interaction between the effect of speed and foot-strike on the aforementioned frequencies. Pairwise post-hoc comparisons using the Tukey HSD test, indicated that significant difference on the pelvis f_c exists solely between the 2.5 and 4.5 m/s conditions (Table 1: in bold; $p = 0.03$). Lastly, there were no significant main effects nor an interaction of either factor on the thigh masses.

Vertical GRFs were then estimated for the validation dataset with the following parameters: 6 Hz for the pelvis f_c of the 2.5 and 3.5 m/s running trials, and 7 Hz for the 4.5 m/s recordings; 20 and 24 Hz for the thigh f_c for the forefoot and rearfoot strikers, respectively (data not shown); thigh masses equal to 14% of each participant's BM. Similarly to the grid-search analysis, RMSE and absolute peak error values decline while speed increases (Table 2). Errors for the second part of our analysis, when averaged for the three speed conditions (0.14 ± 0.04), did not change notably compared to the analogous values from the grid-search (0.13 ± 0.04). One-way ANOVAs were conducted to compare the performance of the validation to the grid-search results. Shapiro-Wilk tests of residuals and Levene's test for homogeneity were carried out and the assumptions were met. There was no statistically significant difference between the two approaches on the quality of the GRF estimation for both RMSE ($p = 0.39$) and absolute peak error values ($p = 0.11$).

Measured and predicted waveforms of the validation set, were divided into six groups as per the trials' running speed and heel-strike pattern. Subsequently, the measured (Fig. 1, solid line) and the predicted (dashed line) vertical GRFs were standardised to BW and normalised to 100% of stance phase (foot-strike to toe-off). Stance phases for each group were then averaged, along with their RMSEs (BW normalised). Reaction forces depicted in cases C and E (forefoot strikers at 3.5 and 4.5 m/s, respectively) bear high RMSEs, however, they incorporate readings from only a single recording each. It is worth noting that every recorded trial contains a number of stances ranging approximately from 75 to 95, depending on subject and running speed. Finally, since the displayed GRFs are an overlay of hundreds of stance phases (Fig. 1, legend), the impact peak appears rather flattened. To better demonstrate the accurate graphical estimation of the double-peak force curves of our model, Fig. 2 shows the average predictions (similarly standardised and normalised as above) for only the first subject of the validation set (i.e. subject 15) in all three speed conditions.

Table 2
Errors (SD) for the validation set.

	RMSE *BW*	Absolute peak error *BW*	R^2
2.5 m/s	0.10 (0.02)	0.06 (0.04)	0.99
3.5 m/s	0.13 (0.03)	0.08 (0.06)	0.99
4.5 m/s	0.18 (0.03)	0.12 (0.08)	0.99
All speeds, m/s	0.14 (0.04)	0.09 (0.07)	0.99

5. Discussion

A straightforward computational Newtonian approach was formulated, with the kinematics of the pelvis and thighs being incorporated into the model. The grid-search led to the identification of factors that reduced the overall errors in the prediction of running GRFs (Table 2). In view of the positive outcomes of our analysis, this class of methods may potentially be used in diverse highly dynamic scenarios, or eventually, in outdoor settings with the use of wearable IMUs.

Alternative methods, including neural networks (e.g. Ngoh et al., 2018; Komaris et al., 2019) and mass-spring-damper models (e.g. Nikooyan & Zadpoor, 2011; Nedergaard et al., 2018) have also adequately predicted the GRFs' vertical projection. Machine learning models may offer a very potent alternative, but they fail to explain the underlying relationship between kinematics and kinetics. Furthermore, they demand large sample sizes to train and provide reliable results. Conversely, mass-spring-damper models were able to justify the behavior of GRF waveforms retrospectively. Besides, those models tend to be accompanied by high complexity when they attempt to incorporate variables, such as running speed, footwear type, or ground stiffness (Nikooyan & Zadpoor, 2011).

Approximated GRF waveforms in this study are rather accurate when compared to other literature reported estimations. The RMS error for low speeds (Table 2, 2.5 m/s) was on average equal to 0.10, and 0.13 to 0.18 for fast-paced running (3.5 and 4.5 m/s, respectively). Previous authors attained RMSEs varying from 0.23 to 0.31 for different running conditions (Ohtaki et al., 2001). Verheul et al. (2018) also reported normalised RMSEs from 0.16 (2–3 m/s) to 0.25 (4–5 m/s); yet, the authors in this study aimed to estimate the resultant reaction force which is accompanied by larger errors due to the inclusion of shearing forces. Lastly, Clark et al. (2017) reported RMSE equal to 0.17 ± 0.07 for all speed conditions (3–6 m/s); despite the fact that the two-mass model presented in the study always assumes a steady-speed level

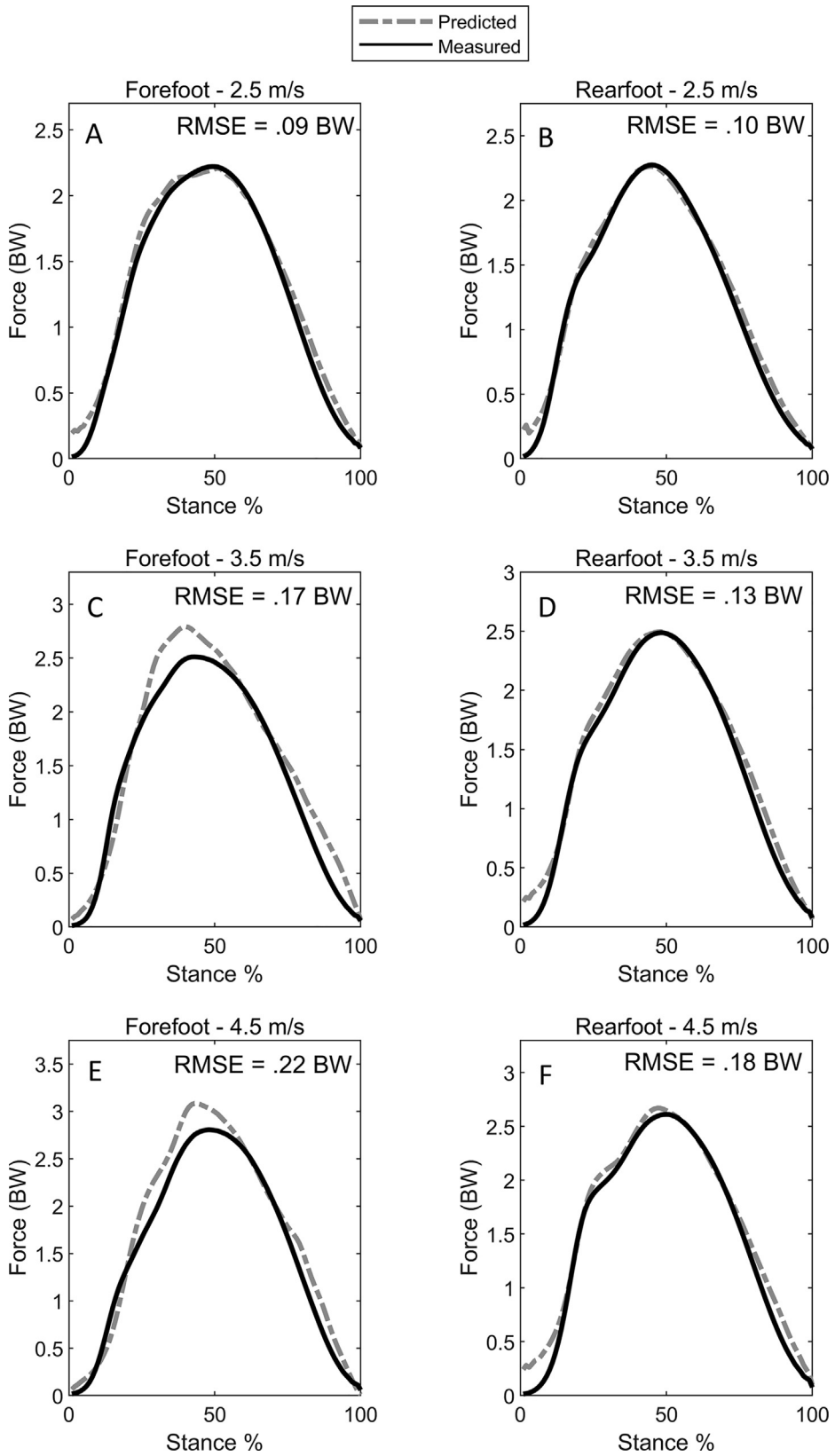

Fig. 1. Measured and estimated vertical ground reaction forces of the validation set. Trials are divided based on running speed and heel strike pattern. Forces are standardised to body weight (BW) and normalised to 100 points. Measured (solid line) and model-predicted (dashed line) waveforms are the average of all stance phases for each speed/foot strike case. The waveform portrayed on panel A (forefoot, 2.5 m/s) is the sum of 3 trials and 235 stance phases. Similarly, panel B (rearfoot, 2.5 m/s): 11 trials and 885 stances; C (forefoot, 3.5 m/s): 1 trial and 82 stances; D (rearfoot, 3.5 m/s): 13 trials and 1111 stances; E (forefoot, 4.5 m/s): 1 trial and 87 stances; F (rearfoot, 4.5 m/s): 13 trials and 1208 stances.

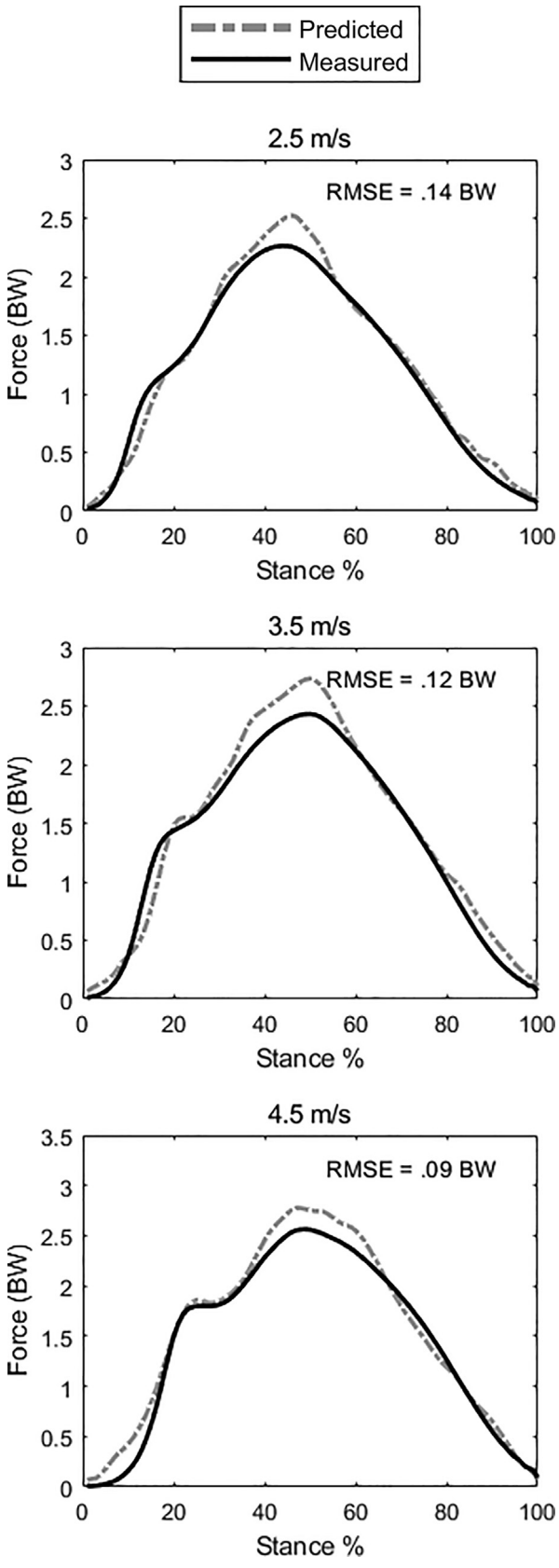

Fig. 2. Measured (solid line) and estimated (dashed line) vertical ground reaction forces of the first subject of the validation set, along with the RMSEs of the predictions. Forces are standardised to body weight (BW) and normalised to 100 points.

running (thus being impractical for other than treadmill applications), it has the added merit of only employing two markers.

In general, a number of factors may account for errors in estimating GRFs from kinematic data. These include the body's mass allocation, filtering of kinematic data, number and combination of sensors and/or segments, and no less importantly, soft tissue artefacts and sensor positioning. The purpose of this work was to investigate the first two: the impact of segmental mass distribution and the filter's f_c in the approximation of running loads. We performed a grid-search where thigh masses from 8% to 28% of total body mass were considered. As hypothesised, this procedure found a consistent mass of 14% *BW* across all conditions and running speeds (Table 1). Interestingly, this percentage does not always agree with literature reported values: Damavandi et al. (2009) defined the greater trochanter and the femoral epicondyle as the thigh boundaries, and the reported mass (normal morphological group, BMI 23.9 kg/m^2) was on average equal to 11.22% (±1.23%) of BW. Drillis et al. (1964) and Winter (2009) also report comparable anthropometrics. However, our findings are in better agreement with the corresponding values reported by De Leva (1996): in this study, thigh length was defined as the distance between iliospinale and tibiale, and the thigh mass was on average equal to 14.16% BW (males, BMI 24.1 kg/m^2). Therefore, taking into account standardised segment masses as reported in literature should be dealt with caution.

As regards the filtering, authors select various f_c for the processing of kinematic data: Clark et al. (2017) and Udofa et al. (2016) applied a low-pass, 4th order, zero-phase-shift Butterworth filter with an f_c of 25 Hz. Yet, as previously reported (Bobbert et al., 1991), when the f_c is set below 10 Hz for all markers the first peak of the curve is flattened, whereas for high f_c the predicted waveform exhibits large fluctuations. Due to this, the use of different f_c for all considered segments leads to predictions that conform better to the measured forces: Bobbert et al. (1991) employed the same filter as Clark et al. but with 50 and 15 Hz f_c for lower and upper-body markers, respectively; Verheul et al. (2018) used a 2nd order Butterworth low-pass filter with 20 and 10 Hz f_c for different segments. In our study, we likewise deduced that different f_c for the upper and lower-body markers optimise the GRFs' estimation for the dataset in hand. Furthermore, as hypothesized, the f_c of the thigh markers tends to marginally increase with higher running speeds.

The number and combination of segments taken into account may also be critically reviewed. Specifically for open field applications, the number of deployed sensors should be kept at a minimum. Then again, reducing the number of the considered segments will significantly increase the errors in estimating GRFs. Indeed, studies assessing a single body segment were accompanied by high RMSE (e.g. Raper et al., 2018; Nedergaard et al., 2018). Verheul et al. (2018) additionally demonstrated that during high intensity running tasks, the errors substantially increase if the number of incorporated segments is reduced below three. Nonetheless, Clark et al. (2017) used merely two ankle markers with robust results for slow and medium running speeds. In terms of combinations of segments, previous studies concur that the main contributors to the first impact peak in the vertical GRFs (when present) are the leg segments, while the remaining masses contribute to the second peak of the waveform (Bobbert et al., 1991; Clark et al., 2017). To further support this argument, Verheul et al. (2018) examined over 32,000 unique segment combinations for the estimation of GRFs, and the trunk and thigh (s) were always present in every optimal combination of two or more segments. On those grounds, in the present study, we merely

considered three segments: the lower-limbs were represented by the thighs, while the remaining masses were treated along with the pelvis. The reader should also keep in mind that the dataset used for this work (Fukuchi et al., 2017) contains only kinematics of the lower extremities, therefore the torso was substituted by the pelvis.

A critical assumption in the approximation of forces from kinematics is that the considered accelerations correspond to segmental COM accelerations. Yet, a segment's COM is not fixated in an anatomical position, and its acceleration emanates from the movement of bony structures and soft tissues (Bobbert et al., 1991). Therefore, the presence of soft tissue artefacts and poor sensor positioning may introduce high computational errors in such analyses. It has been demonstrated (Boyer & Nigg, 2004; Schache et al., 2011) that high running speeds were accompanied by larger soft tissue vibrations and errors in kinematic calculations. This is even apparent in the present study, where RMSEs increase substantially during fast-paced running (Tables 1 and 2). Similarly, poor sensor placement (Leardini et al., 2005) may also have a negative impact: Reinschmidt et al. (1997) and Peters et al. (2010) observed errors when markers were placed on large muscles due to intense muscle activity and relative movements. This is particularly evident with the tracking of thigh markers (Reinschmidt et al., 1997; Peters et al., 2010); for this, it is advised to restrict marker placement to areas with lower muscle contractions, such as the anterolateral part of the distal third of the thigh (Schache et al., 2011).

A limitation of this study is imposed by the number of markers used in the analysis. Ideally, only a marker per segment should be considered allowing the applicability of the findings to be extended to IMUs. Instead, four pelvis markers and two thigh clusters were used. By all means, employing more markers per segment permits a more accurate estimation of the segment's COM location, and consequently, more precise GRF estimations. Thus, it can be reasonably expected that reducing the number of markers to one per segment will return higher RMSE values. A second limitation of this work arises from the use of only 2nd order filters; even though Butterworth was the prevalent choice by researchers who worked on the prediction of GRFs from human kinematics, the order of the employed filter may extend from 2nd (e.g. Karatsidis et al., 2016; Pavei et al., 2017; Verheul et al., 2018; Komaris et al., 2019) to 4th (e.g. Udofa et al., 2016; Clark et al., 2017; Nedergaard et al., 2018; Shahabpoor & Pavic, 2018). Since the order alters the amplitude response in both passband and stopband, the output signal may be significantly affected by this parameter; therefore, our optimisation holds true only for 2nd order filters. Lastly, anatomical differences between males and females were not been taken into account in this work. Even though there is a relatively little difference in the thighs' segment mass between sexes (as reported by De Leva, 1996: 14.78% and 14.16% of BW for females and males, respectively), we were unable to gauge the effect of sex in segment mass distribution since only one female subject was included in the employed dataset (Fukuchi et al., 2017).

6. Conclusion

This study demonstrated that accurate prediction of vertical GRFs, for moderate running speeds, can be reasonably achieved with the kinematics of only three segments. The effects of the filter's f_c and body mass distribution on the estimation of the waveforms were also investigated. Findings support the existence of correlations between f_c and two factors: running speed and foot-strike strategies. Optimal segment masses were constant along all tested conditions and in agreement with certain literature reported values. However, researchers should be skeptical when incorporating standardised values for biomechanical models due to the different boundaries used to define segments. Future work should consider the adoption of compensating techniques for the presence of soft tissue artefacts, or the placement of sensors to areas with lower muscle activity.

Data availability

Data available at figsgare (DOI: 10.6084/m9.figshare.4543435).

Declaration of Competing Interest

There are no conflicts of interest to declare.

Acknowledgments

This work was supported in part by the Enterprise Ireland and Setanta College Ltd., under Agreement IP 2017 0606, and in part by the European Regional Development Fund (ERDF) through the Ireland's European Structural and Investment Funds Programmes 2014-2020. Aspects of this publication have emanated from research conducted with the financial support of Science Foundation Ireland under Grant number 12/RC/2289-P2 INSIGHT which is co-funded under the European Regional Development Fund.

References

Ancillao, A., Tedesco, S., Barton, J., O'Flynn, B., 2018. Indirect measurement of ground reaction forces and moments by means of wearable inertial sensors. A systematic review. Sensors (Basel) 18 (8). https://doi.org/10.3390/s18082564.

Bates, N.A., Ford, K.R., Myer, G.D., Hewett, T.E., 2013. Impact differences in ground reaction force and center of mass between the first and second landing phases of a drop vertical jump and their implications for injury risk assessment. J. Biomech. 46 (7), 1237–1241. https://doi.org/10.1016/j.jbiomech.2013.02.024.

Bobbert, M.F., Schamhardt, H.C., Nigg, B.M., 1991. Calculation of vertical ground reaction force estimates during running from positional data. J. Biomech. 24 (12), 1095–1105.

Boyer, K.A., Nigg, B.M., 2004. Muscle activity in the leg is tuned in response to impact force characteristics. J. Biomech. 37 (10), 1583–1588. https://doi.org/10.1016/j.jbiomech.2004.01.002.

Chmielewski, T.L., Myer, G.D., Kauffman, D., Tillman, S.M., 2006. Plyometric exercise in the rehabilitation of athletes: physiological responses and clinical application. J. Orthop. Sports Phys. Ther. 36 (5), 308–319.

Clark, K.P., Ryan, L.J., Weyand, P.G., 2017. A general relationship links gait mechanics and running ground reaction forces. J. Exp. Biol. 220 (Pt 2), 247–258. https://doi.org/10.1242/jeb.138057.

Clauser, C.E., McConville, J.T., Young, J.W., 1969. Weight, volume, and center of mass of segments of the human body: Antioch Coll Yellow Springs OH.

Crea, S., Donati, M., De Rossi, S.M.M., Oddo, C.M., Vitiello, N., 2014. A Wireless flexible sensorized insole for gait analysis. Sensors (Basel) 14 (1), 1073–1093.

Dainis, A., 1980. Whole body and segment center of mass determination from kinematic data. J. Biomech. 13 (8), 647–651. https://doi.org/10.1016/0021-9290(80)90350-4.

Damavandi, M., Farahpour, N., Allard, P., 2009. Determination of body segment masses and centers of mass using a force plate method in individuals of different morphology. Med. Eng. Phys. 31 (9), 1187–1194. https://doi.org/10.1016/j.medengphy.2009.07.015.

De Leva, P., 1996. Adjustments to Zatsiorsky-Seluyanov's segment inertia parameters. J. Biomech. 29 (9), 1223–1230.

Drillis, R., Contini, R., Bluestein, M., 1964. Body segment parameters; a survey of measurement techniques. Artif. Limbs. 8, 44–66.

El Kati, R., Forrester, S., Fleming, P., 2010. Evaluation of pressure insoles during running. Procedia Eng. 2 (2), 3053–3058. https://doi.org/10.1016/j.proeng.2010.04.110.

Fluit, R., Andersen, M.S., Kolk, S., Verdonschot, N., Koopman, H.F.J.M., 2014. Prediction of ground reaction forces and moments during various activities of daily living. J. Biomech. 47 (10), 2321–2329. https://doi.org/10.1016/j.jbiomech.2014.04.030.

Fong, D.T.-P., Chan, Y.-Y., Hong, Y., Yung, P.S.-H., Fung, K.-Y., Chan, K.-M., 2008. Estimating the complete ground reaction forces with pressure insoles in walking. J. Biomech. 41 (11), 2597–2601. https://doi.org/10.1016/j.jbiomech.2008.05.007.

Forner Cordero, A., Koopman, H.J.F.M., van der Helm, F.C.T., 2004. Use of pressure insoles to calculate the complete ground reaction forces. J. Biomech. 37 (9), 1427–1432. https://doi.org/10.1016/j.jbiomech.2003.12.016.

Fukuchi, R.K., Fukuchi, C.A., Duarte, M., 2017. A public dataset of running biomechanics and the effects of running speed on lower extremity kinematics and kinetics. PeerJ 5, e3298. https://doi.org/10.7717/peerj.3298.

Gurchiek, R.D., McGinnis, R.S., Needle, A.R., McBride, J.M., van Werkhoven, H., 2017. The use of a single inertial sensor to estimate 3-dimensional ground reaction force during accelerative running tasks. J. Biomech. 61, 263–268. https://doi.org/10.1016/j.jbiomech.2017.07.035.

Jacobs, D.A., Ferris, D.P., 2015. Estimation of ground reaction forces and ankle moment with multiple, low-cost sensors. J. NeuroEng. Rehab. 12 (1), 90. https://doi.org/10.1186/s12984-015-0081-x.

Karatsidis, A., Bellusci, G., Schepers, H.M., de Zee, M., Andersen, M.S., Veltink, P.H., 2016. Estimation of ground reaction forces and moments during gait using only inertial motion capture. Sensors (Basel) 17 (1). https://doi.org/10.3390/s17010075.

Kawamori, N., Nosaka, K., Newton, R.U., 2013. Relationships between ground reaction impulse and sprint acceleration performance in team sport athletes. J. Strength Condi. Res. 27 (3), 568–573. https://doi.org/10.1519/JSC.0b013e318257805a.

Kohle, M., Merkl, D., & Kastner, J. (1997, 11–13 June 1997). Clinical gait analysis by neural networks: issues and experiences. Paper Presented at the Proceedings of Computer Based Medical Systems.

Komaris, D.S., Perez-Valero, E., Jordan, L., Barton, J., Hennessy, L., O'Flynn, B., Tedesco, S., 2019. Predicting three-dimensional ground reaction forces in running by using artificial neural networks and lower body kinematics. IEEE Access 7. 10.1109/ACCESS.2019.2949699. doi: https://doi.org/10.1109/ACCESS.2019.2949699.

Leardini, A., Chiari, L., Della Croce, U., Cappozzo, A., 2005. Human movement analysis using stereophotogrammetry. Part 3. Soft tissue artifact assessment and compensation. Gait Posture 21 (2), 212–225. https://doi.org/10.1016/j.gaitpost.2004.05.002.

Liedtke, C., Fokkenrood, S.A.W., Menger, J.T., van der Kooij, H., Veltink, P.H., 2007. Evaluation of instrumented shoes for ambulatory assessment of ground reaction forces. Gait & Posture 26 (1), 39–47. https://doi.org/10.1016/j.gaitpost.2006.07.017.

Nedergaard, N.J., Verheul, J., Drust, B., Etchells, T., Lisboa, P., Robinson, M.A., Vanrenterghem, J., 2018. The feasibility of predicting ground reaction forces during running from a trunk accelerometry driven mass-spring-damper model. PeerJ 6, e6105. https://doi.org/10.7717/peerj.6105.

Ngoh, K.J., Gouwanda, D., Gopalai, A.A., Chong, Y.Z., 2018. Estimation of vertical ground reaction force during running using neural network model and uniaxial accelerometer. J. Biomech. 76, 269–273. https://doi.org/10.1016/j.jbiomech.2018.06.006.

Nikooyan, A.A., Zadpoor, A.A., 2011. Mass-spring-damper modelling of the human body to study running and hopping – an overview. Proc. Inst. Mech. Eng. H 225 (12), 1121–1135. https://doi.org/10.1177/0954411911424210.

Oh, S.E., Choi, A., Mun, J.H., 2013. Prediction of ground reaction forces during gait based on kinematics and a neural network model. J. Biomech. 46 (14), 2372–2380. https://doi.org/10.1016/j.jbiomech.2013.07.036.

Ohtaki, Y., Sagawa, K., Inooka, H., 2001. A method for gait analysis in a daily living environment by body-mounted instruments. JSME Int. J. Series C 44 (4), 1125–1132. https://doi.org/10.1299/jsmec.44.1125.

Pavei, G., Seminati, E., Storniolo, J.L., Peyre-Tartaruga, L.A., 2017. Estimates of running ground reaction force parameters from motion analysis. J. Appl. Biomech. 33 (1), 69–75. https://doi.org/10.1123/jab.2015-0329.

Peters, A., Galna, B., Sangeux, M., Morris, M., Baker, R., 2010. Quantification of soft tissue artifact in lower limb human motion analysis: a systematic review. Gait Posture 31 (1), 1–8. https://doi.org/10.1016/j.gaitpost.2009.09.004.

Raper, D.P., Witchalls, J., Philips, E.J., Knight, E., Drew, M.K., Waddington, G., 2018. Use of a tibial accelerometer to measure ground reaction force in running: a reliability and validity comparison with force plates. J. Sci. Med. Sport 21 (1), 84–88. https://doi.org/10.1016/j.jsams.2017.06.010.

Reinschmidt, C., van den Bogert, A.J., Nigg, B.M., Lundberg, A., Murphy, N., 1997. Effect of skin movement on the analysis of skeletal knee joint motion during running. J. Biomech. 30 (7), 729–732.

Ren, L., Jones, R.K., Howard, D., 2008. Whole body inverse dynamics over a complete gait cycle based only on measured kinematics. J. Biomech. 41 (12), 2750–2759. https://doi.org/10.1016/j.jbiomech.2008.06.001.

Schache, A.G., Blanch, P.D., Dorn, T.W., Brown, N.A., Rosemond, D., Pandy, M.G., 2011. Effect of running speed on lower limb joint kinetics. Med. Sci. Sports Exerc. 43 (7), 1260–1271. https://doi.org/10.1249/MSS.0b013e3182084929.

Shahabpoor, E., Pavic, A., 2017. Measurement of walking ground reactions in real-life environments: a systematic review of techniques and technologies. Sensors (Basel) 17 (9). https://doi.org/10.3390/s17092085.

Shahabpoor, E., Pavic, A., 2018. Estimation of vertical walking ground reaction force in real-life environments using single IMU sensor. J. Biomech. 79, 181–190. https://doi.org/10.1016/j.jbiomech.2018.08.015.

Shu, L., Hua, T., Wang, Y., Li, Q., Feng, D.D., Tao, X., 2010. In-shoe plantar pressure measurement and analysis system based on fabric pressure sensing array. IEEE Trans. Inf Technol. Biomed. 14 (3), 767–775. https://doi.org/10.1109/TITB.2009.2038904.

Tao, W., Liu, T., Zheng, R., Feng, H., 2012. Gait analysis using wearable sensors. Sensors (Basel, Switzerland) 12 (2), 2255–2283. https://doi.org/10.3390/s120202255.

Tedesco, S., Urru, A., Clifford, A., O'Flynn, B., 2016. Experimental validation of the tyndall portable lower-limb analysis system with wearable inertial sensors. Procedia Eng. 147, 208–213. https://doi.org/10.1016/j.proeng.2016.06.215.

Udofa, A.B., Ryan, L.J., Weyand, P.G., 2016, 14–17 June 2016. Impact forces during running: Loaded questions, sensible outcomes. Paper presented at the 2016 IEEE 13th International Conference on Wearable and Implantable Body Sensor Networks (BSN).

Verheul, J., Gregson, W., Lisboa, P., Vanrenterghem, J., Robinson, M.A., 2018. Whole-body biomechanical load in running-based sports: The validity of estimating ground reaction forces from segmental accelerations. J. Sci. Med. Sport. https://doi.org/10.1016/j.jsams.2018.12.007.

Winter, D.A., 2009. Biomechanics and Motor Control of Human Movement. John Wiley & Sons.